Physical Modelling in Geotechnics
© 2022 KOREAN GEOTECHNICAL SOCIETY (KGS), Seoul, Korea, ISBN 978-89-952197-7-5

Tracking seismically-induced embankment deformations using high-speed camera arrays and PIV in a large centrifuge model

N.C. Love, J.T. DeJong & D.W. Wilson
Department of Civil & Env. Engineering, University of California at Davis, USA

T.J. Carey
Department of Civil Engineering, The University of British Columbia, Canada

ABSTRACT: Accurate measurement of embankment deformations during centrifuge tests is a persistent challenge. For large centrifuge model containers, such as the 1.75 m long container used on the 9-m-radius centrifuge at the UC Davis Center for Geotechnical Modeling (CGM), multiple cameras or sensors are needed to achieve the measurement coverage and accuracy required for engineering analysis. The tracking process described herein, including hardware and procedures, addresses this challenge. Three synchronized high-speed cameras positioned on the exterior of a model container record deformations of submerged sloping embankments during strong shaking as viewed through the clear polycarbonate longitudinal sidewalls of the model container. Vertical black sand columns installed between the model cross-section and container sidewalls were used for visual tracking of embankment deformations. Displacement time-series were generated for the four events of the shaking sequence using an overlapping mesh of GEOPIV-RG patches defined for each black sand column. The measured deformations from GEOPIV-RG, confirmed with manual measurements of the free-field conditions following testing, showed that the black sand columns deformed with the embankment cross-sections. While GEOPIV-RG has traditionally been used to track micro particle movements, the multiple cameras and their positioning used herein enabled the measurement of accumulating system level deformations across the global failure mechanism. These results have provided valuable insights into embankment system performance when subjected to shaking.

Keywords: Liquefaction embankment deformation, Centrifuge experiments, PIV, High-speed cameras, Displacement tracking

1 INTRODUCTION

Tracking deformations in dynamic centrifuge experiments is a difficult task. In the past, researchers have used contacting sensors such as Linear Variable Differential Transformers (LVDTs); however, the sensors can reinforce the soil and resist deformations (Fiegel and Kutter, 1994). More recently, a method that tracks surface markers from above slopes using high-speed cameras and particle image velocimetry (PIV) was developed (Carey et. al., 2018). However, this method requires visibility of the slope surface and does not capture deformations within an embankment. Kennedy et al. (2021) uses GEOPIV to track retrogressive landslide events with a single camera per slope.

This paper presents a new method to track embankment deformations of a model cross section with multiple high-speed cameras and PIV software. High-speed cameras were positioned along the exterior of a model container recording plane strain deformations of the visible cross-section through clear polycarbonate container sidewalls. The recorded images were processed using GEOPIV-RG (Stanier et al., 2015) to obtain displacement time histories. While PIV has traditionally been used to track granular movements using a single camera, the use of multiple cameras to create a wider field of view herein allowed for tracking deformations across the system level failure mechanism.

2 TEST PROGRAM AND MODEL CONFIGURATION

A centrifuge testing program was undertaken to compare the dynamic system-level response of embankments constructed of sands with different gradations. The testing program consisted of four sands, Sands A, B, C, and D, which were progressively more well-graded and differed in their physical properties. The experiment was designed with two geometrically identical embankments, positioned side-by-side and pluviated to the same relative density, but differing in sand type. The experiments were performed at 40-times-gravity and subjected to four strong motion shaking events. The applied motion was a 1-Hz (prototype scale)

non-uniform sine wave. The shaking intensity increased from 0.1 g in the first shake to 0.4 g in the last shake. The embankment response was recorded using embedded vertical arrays of accelerometers and porewater pressure transducers. An external system of high-speed cameras captured images through the clear sidewalls. For more details regarding the testing program, the reader is directed to Carey et al. (2022) (Sand A = 100A and Sand C = 25ABCD).

The model was designed for the 1.75 m long rigid container for the 9-m-radius centrifuge at the UC Davis Center for Geotechnical Modeling (CGM). The model cross-section is shown in Fig.1. The two embankments were separated by an aluminum wall that split the container into two equal widths. The embankments had level ground at the head and toe, joined by a 10 degree slope. A 50 mm thick dense sand base layer was used to raise the embankments into the fields of view of the cameras. The embankments were saturated and submerged with a viscous pore fluid of μ*=40.

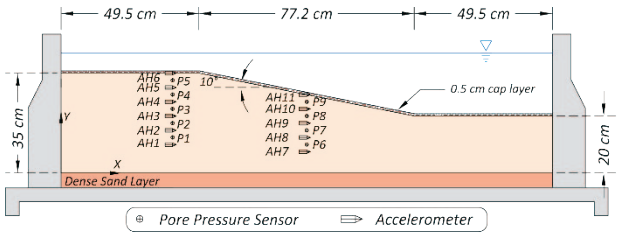

Fig. 1. Elevation view of model experiment configuration.

Vertical columns of dyed sand were developed to visualize embankment deformations. From the camera positions, the embankment sand was too uniform in color and texture for PIV to reliably track displacements. Black sand columns that contrasted with the surrounding soil were added to enable accurate PIV analysis. The columns were made by mixing embankment sand dyed with black paint with water-soluble glue in a 1:2.5 (glue:sand) ratio by mass. The uniform mixture was placed into a mold with 12-mm-deep grooves, partially dried overnight, removed and trimmed to be approximately 6 mm thick so as to not obstruct the pluviation process, and then fully dried. White lines were drawn onto the columns with an oil-based paint marker, spaced at 1 cm and angled 45 degrees from horizontal. The black sand columns were sealed to the clear container sidewalls using a mixture of undyed sand and glue prior to pluviation to prevent pluviated sand from obstructing the view of the columns. Once saturated, the glue dissolved, leaving vertical colored sand lines that did not reinforce the embankments.

PIV requires static reference seed points to measure relative displacements of a PIV patch. Seed points were designed with three concentric circles, alternating white and black, whose diameters were roughly 0.8, 2.5 and 7.5 mm. Two seed points per camera were adhered to the exterior of the container sidewall in the bottom third of the camera's field of view where the deformations would be smaller, just upslope of the nearest sand column. This location allowed for significant deformation of the upslope adjacent sand column before obstructing its view.

3 HIGH-SPEED CAMERAS

Three high-speed cameras were positioned outside the model container along each sidewall to record the cross-sectional embankment deformations during shaking. The cameras were spaced 31 cm from the container walls and positioned with overlapping fields of view, as indicated in Fig. 2. The cameras were mounted directly to the centrifuge shake table, such that soil movements were recorded relative to the container, cameras, and input shaking. The lighting system (upper and base lighting) was designed to provide indirect illumination of the slopes to minimize glare from direct lighting. The camera heads were controlled from a central computer, enabling time-synchronized automatic recording. Each camera was equipped with a 6 mm fixed focal length lens.

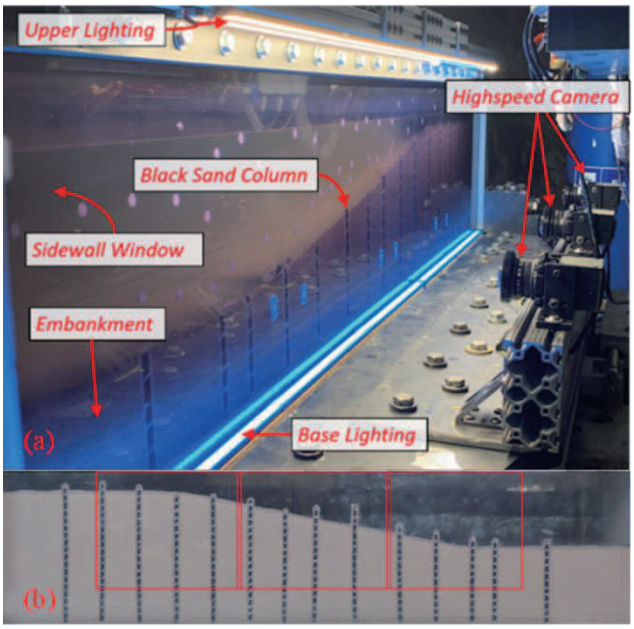

Fig. 2. (a) Model container on the centrifuge arm, with components indicated: lighting, black sand columns, sidewall window, high-speed cameras, and embankment (Carey et al., 2022) (b) Constructed embankment viewed through the clear container sidewall with camera fields of view indicated.

The central computer utilized proprietary image acquisition software to control the cameras. The chosen framerate of 1000 frames per second (fps) resulted in 25 frames per cycle of loading given the applied 40 Hz shaking motion (model scale). The recording resolution was set to 1280×1024 pixels (px). Lens distortion was corrected using built-in functionality of the image acquisition software. Since the cameras were positioned

© 2022 KOREAN GEOTECHNICAL SOCIETY (KGS), Seoul, Korea, ISBN 978-89-952197-7-5

the same distance from the container sidewall, used the same lenses, and were recording a planar surface, a single lens correction calibration was used for all cameras.

4 IMAGE PROCESSING WITH GEOPIV-RG

The images captured during shaking were processed with GEOPIV-RG. A custom mesh of PIV patches that overlapped the black sand columns was defined. The Eulerian analysis technique, which automatically updated the 'reference' image using the recommended values for the secondary parameters, was used. The tracked patch locations were plotted on the corresponding image to visually verify tracking agreement. This additional step increased confidence in the image processing results, with a negligible computational cost.

GEOPIV-RG outputs patch locations for each frame in px, which were then converted to engineering units (mm). Calibration factors were determined by capturing images of a calibration checkerboard taped to the inside wall of the container window. A conversion factor was determined for each sand column location, using the number of px that spanned the known width of calibration checker at the locations where the columns would be in the image. The average factor was about 3.2 px/mm.

5 RESULTS AND DISCUSSION

A subset of results from the GEOPIV-RG analysis of the images captured during shaking are presented and discussed herein.

By tracking discrete columns with known model locations, results across multiple cameras were combined into a single embankment representation. Fig. 3 presents a deformation quiver plot for a single shaking event. Permanent deformations include both horizontal and vertical components that accumulated during a single shaking event, and a vector corresponding to 1 m of displacement is included above the figure for scale.

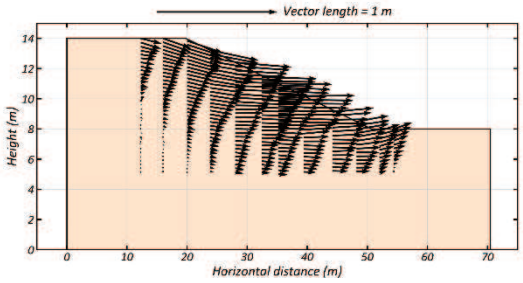

Fig. 3. Deformation quiver plot for Shake 2 of embankment B.

For each PIV patch (corresponding to a single vector in Fig. 3), the dynamic and cumulative deformations were evaluated. Fig. 4 shows the horizontal displacements for all shaking events for the PIV patches co-located with accelerometers AH5 (left) and AH10 (right) (see Fig. 1 for sensor locations). The dynamic deformations, seen mostly clearly as the sinusoidal variations during Shake 4, demonstrate how embankment deformations accumulate and are resisted during cyclic loading.

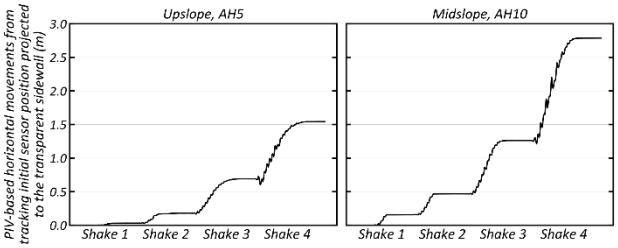

Fig. 4. Cumulative horizontal displacements for all shaking events for the patches co-located with sensors AH5 (left) and AH10 (right). Each subsequent shaking motion increased in intensity, resulting in an increase in displacements.

The variation in deformation across the 434 mm width of the embankment was evaluated by comparing the cumulative horizontal displacements measured at the container boundary using PIV analysis (i.e., the maximum value in Fig. 4) to the before and after positions of buried sensors located at the center of the model, determined by manual measurements during model construction and dissection. The result of this comparison is presented in Fig. 5, which shows reasonable agreement between the PIV analysis-based displacements and manual displacement measurements for multiple experiments, soil types, and model locations. The data is slightly biased to higher displacements from hand measurements. However, this is consistent with PIV measurements only capturing deformations from shaking, while neglecting other events that could induce model disturbance, including model transportation, saturation, and drawdown/desaturation. Previous researchers have observed that deformations along the edges may be reduced compared to the center cross-section due to boundary interactions between the soil and model container sidewalls (e.g., Madabhushi et al., 2018). However, any difference due to the boundary constraint was observed to be too small to be reliably differentiated in this set of experiments.

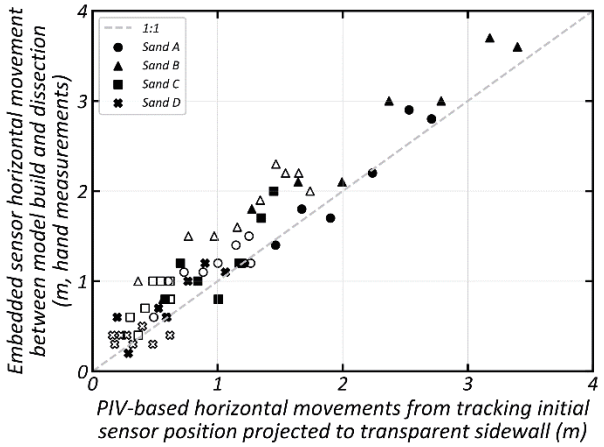

Fig. 5. Comparison of horizontal displacements measured by PIV compared to hand measurements of sensor locations, for all sensors in the upslope (open symbol) and downslope (closed symbol) array and their corresponding PIV patches.

6 CONCLUSIONS

Novel hardware and procedures were developed to track liquefaction-induced plane-strain embankment deformations across the depth of a centrifuge model. Six high-speed cameras were positioned along the clear sidewalls of a rigid model container to track movements in two geometrically similar slopes. Vertical columns of dyed sand were used to add visual contrast for tracking deformations of the embankments. Indirect lighting was placed above and below the window to illuminate the embankment while minimizing glare. Displacement time histories were generated using the captured images and GEOPIV-RG software. The following conclusions were drawn from this method:

- The nuances of the model setup (e.g., lighting, seed points, coloring of columns, etc.) facilitated accurate tracking of embankment deformations.
- Plotting the recorded patch locations on the image proved to be a useful method to confirm that GEOPIV-RG tracked observed displacements.
- The black sand columns minimized invasiveness (i.e., did not obstruct pluviation or make loose pockets of sand) and, being made of the same in-situ material, minimized influence on the embankment response. Further, the water-soluble glue dissolved during saturation and thus did not reinforce the slopes.
- By tracking the deformations of discrete sand columns, incremental deformations across multiple cameras could be combined into a single embankment representation.
- Using three high-speed cameras per embankment to capture deformations enabled the use of a larger model container with denser arrays of sensors that influence the overall response less than smaller models and captured the system-level response of the entire embankment.
- While there were unavoidable boundary interactions between the model container sidewall and the embankment, a comparison between hand measurements of sensors located at the center of the model to the corresponding PIV patches on the side windows showed good agreement.

ACKNOWLEDGEMENTS

Research was supported by the National Science Foundation (NSF) under CMMI-1916152. Operation of the centrifuge at UC Davis was supported by NSF through the Natural Hazards Engineering Research Infrastructure (NHERI) program under CMMI-1520581. The authors would like to thank Tom Kohnke, Chad Justice, and Anatoliy Ganchenko for their assistance during planning and testing.

REFERENCES

Carey, T. J., Chiaradonna, A., Love, N. C., Wilson, D. W., Ziotopoulou, K., Martinez, A., and DeJong, J. T. (2022). Effect of soil gradation on embankment response during liquefaction: a centrifuge testing program. *Soil Dynamics and Earthquake Engineering* (submitted 11/2021).

Carey, T. J., Stone N., Kutter, B. L., and Hajialilue-Bonab, M. (2018). A new procedure for tracking displacements of submerged sloping ground in centrifuge testing. *Proceedings 9th International Conference on Physical Modeling in Geotechnics (ICPMG 2018)*, London, UK, 829–834.

Fiegel, G. L. and Kutter, B. L., (1994). Liquefaction mechanism for layered soils. *Journal of geotechnical engineering*, 120(4), pp. 737–755.

Kennedy, R., Take, W. A., & Siemens, G. (2021). Geotechnical centrifuge modelling of retrogressive sensitive clay landslides. Canadian Geotechnical Journal, 58(10), 1452-1465.

Madabhushi, S., Haigh, S., and Madabhushi, G. (2018). LEAP-GWU-2015: Centrifuge and numerical modelling of slope liquefaction at the University of Cambridge. *Soil Dynamics and Earthquake Engineering* doi: 10.1016/j.soildyn.2016.11.009.

Stanier, S. A., Blaber, J., Take, W. A., and White, D. J. (2015). "Improved image-based deformation measurement for geotechnical applications." *Canadian Geotechnical Journal*, 53: 727-739. doi: 10.1139/cgj-2015-0253.